

**Working Title: Monte Carlo Analysis of Dynamic Systems**

by

Chelsea A. D'Angelo

A preliminary report submitted in partial fulfillment of  
the requirements for the degree of

Doctor of Philosophy

(Nuclear Engineering and Engineering Physics)

at the

UNIVERSITY OF WISCONSIN-MADISON

2017

Date of preliminary oral examination: 09/01/2017

Thesis Committee:

Paul P. H. Wilson, Professor, Nuclear Engineering

Douglass Henderson, Professor, Nuclear Engineering

Bryan Bednarz, Professor, Medical Physics

Andrew Davis, Associate Scientist, Engineering Physics



© Copyright by Chelsea A. D'Angelo 2017  
All Rights Reserved

## CONTENTS

---

Contents	i
List of Figures	iii
<b>1 Introduction</b>	<b>1</b>
<b>2 Literature Review</b>	<b>4</b>
2.1 <i>Analog Monte Carlo Calculations</i> . . . . .	5
2.2 <i>Shutdown Dose Rate Analysis</i> . . . . .	6
2.2.1 D1S . . . . .	6
2.2.2 R2S . . . . .	7
2.3 <i>Monte Carlo Variance Reduction Methods</i> . . . . .	7
2.4 <i>Automated Variance Reduction</i> . . . . .	9
2.4.1 CADIS . . . . .	11
2.4.2 FW-CADIS . . . . .	12
2.5 <i>Automated Variance Reduction for Multiphysics</i> . . . . .	13
2.5.1 MS-CADIS . . . . .	14
2.5.2 GT-CADIS . . . . .	15
2.6 <i>Moving Geometries and Sources</i> . . . . .	16
2.6.1 MCNP6 Moving Objects Capability . . . . .	16
2.6.2 MCR2S with Geometry Movement . . . . .	17
<b>3 Experiment</b>	<b>19</b>
3.1 <i>Demonstration of GT-CADIS</i> . . . . .	19
3.1.1 Problem Description . . . . .	19
3.1.2 Analog R2S . . . . .	20
3.1.3 GT-CADIS . . . . .	21
3.2 <i>Limitations of GT-CADIS for Moving Systems</i> . . . . .	25

<b>4</b>	<b>Variance Reduction for Time-integrated Multiphysics Analysis</b>	<b>32</b>
4.1	<i>Generalized MS-CADIS Method</i> . . . . .	32
4.2	<i>Time-integrated MS-CADIS</i> . . . . .	35
4.3	<i>Time-integrated GT-CADIS</i> . . . . .	36
<b>5</b>	<b>Progress</b>	<b>38</b>
5.1	<i>DAGMC Simulations with Geometry Transformations</i> . . . . .	38
5.1.1	Production of Stepwise Geometry Files . . . . .	38
5.1.2	DAGMCNP Geometry Transformations . . . . .	39
<b>6</b>	<b>Proposal</b>	<b>40</b>
6.1	<i>TR2S</i> . . . . .	40
6.2	<i>Implementation: Time-integrated SDR Analysis</i> . . . . .	41
6.2.1	Generation of the TGT-CADIS Variance Reduction Parameters . . . . .	41
6.2.2	Optimized, Time-integrated R2S Workflow . . . . .	44
6.2.3	Error Propagation . . . . .	46
6.2.4	Assumptions and Practical Considerations . . . . .	48
6.2.4.1	Data management . . . . .	49
6.3	<i>Demonstration</i> . . . . .	50
6.3.1	Toy Problem . . . . .	50
6.3.2	Full-scale FES Model . . . . .	50
6.4	<i>Summary</i> . . . . .	51
	<b>Bibliography</b>	<b>52</b>

## LIST OF FIGURES

---

3.1	Experimental Geometry . . . . .	20
3.2	Analog neutron flux and error . . . . .	22
3.3	Analog photon source . . . . .	23
3.4	GT-CADIS adjoint photon flux . . . . .	24
3.5	GT-CADIS adjoint neutron flux . . . . .	25
3.6	GT-CADIS biased neutron source . . . . .	26
3.7	GT-CADIS weight window mesh . . . . .	27
3.8	GT-CADIS neutron flux and relative error . . . . .	28
3.9	GT-CADIS photon source . . . . .	29
3.10	Path of moving component . . . . .	30
3.11	Adjoint neutron flux, highlighted region of moving component	31
6.1	Time-integrated R2S (TR2S) workflow . . . . .	42
6.2	Workflow to generate TGT-CADIS adjoint neutron source . . .	45
6.3	Workflow to generate TGT-CADIS biased source and weight windows . . . . .	46
6.4	Fully optimized, time-integrated R2S workflow . . . . .	47
6.5	Geometry for TGT-CADIS Demonstration . . . . .	50

## **Abstract**

### **Abstract**

Eloquent summary of my work.

## 1 INTRODUCTION

---

The successful completion of this project will provide the workflow and tools necessary to efficiently calculate quantities of interest resulting from coupled, multi-physics processes in dynamic systems. The MC physics code will be modified to implement rigid-body transformations on the CAD-based geometry. MS-CADIS, a VR method for coupled, multi-physics problems, will be adapted to incorporate dynamics. An experiment will be contrived to demonstrate the limitations of existing VR methods as they apply to dynamic problems and verify the efficacy of this new method. Given these objectives, the following chapters will include background and theory relevant to VR methods in coupled, multi-physics systems. Chapter 2 will provide an introduction to computational radiation transport and specifically the VR methods used in MC calculations. Chapter no. will discuss SDR analysis and the VR methods specific to these calculations. Chapter no. will introduce radiation transport in dynamic systems, discuss how they are handled now and how motion affects VR in coupled multi-physics problems like SDR calculations. Finally, chapter no. will discuss the progress that has been made towards this new methodology and outline a proposal of the work to be done.

The rapid design iteration process of complex nuclear systems has long been aided by the use of computational simulation. Traditionally, these simulations involve radiation transport in static geometries. However, in certain scenarios, it is desirable to investigate dynamic systems and the effects caused by the motion of one or more components. For example, Fusion Energy Systems (FES) are purposefully designed with modular components that can be moved in and out of a facility after shutdown for maintenance. To ensure the safety of maintenance personnel, it is important to accurately quantify the shutdown dose rate (SDR) caused by the gammas emitted by structural materials that became activated during the



device operation time. This type of analysis requires neutron transport to determine the neutron flux, activation calculation to determine the isotopic inventory, and finally a photon transport calculation to determine the SDR. While MC calculations are revered to be the most accurate method for simulating radiation transport, the computational expense of obtaining low error results in systems with heavy shielding can be prohibitive. However there are techniques, known as variance reduction (VR) methods, that can be used to increase the computational efficiency. There are several types of VR methods, but the basic theory is to artificially increase the simulation of events that will contribute to the quantity of interest such as flux or dose rate. One class of VR techniques relies upon a deterministic estimate of the adjoint solution of the transport equation to formulate biasing parameters used in the MC transport. The adjoint flux has physical significance as the importance of a region of phase space to the objective function.

The purpose of this work is to create a methodology for the efficient calculation of quantities of interest in dynamic, geometrically complex nuclear systems. For cases involving coupled multi-physics analysis, such as SDR calculations, a new hybrid deterministic/MC VR technique will be proposed. This new method will adapt the Multi-Step Consistent Adjoint Driven Importance Sampling (MS-CADIS) method to dynamic systems. The basis of MS-CADIS is that the importance function used in each step of the problem must represent the importance of the particles to the final objective function. As the spatial configuration of the materials changes, the probability that they will contribute to the objective function also changes. In the specific case of SDR calculations, the importance function for the neutron transport step must capture the probability of materials to become activated and subsequently emit photons that will make a significant contribution to the SDR. This new VR method will also take advantage of the Groupwise Transmutation (GT)-CADIS method which is an implementation of MS-CADIS that optimizes the neutron transport

step of SDR calculations. GT-CADIS generates an adjoint neutron source based on certain assumptions and approximations about the transmutation network. To adapt this method for dynamic systems, the adjoint neutron source will be calculated at each time step and then averaged in order to generate the biasing functions for the neutron transport step.

## 2 LITERATURE REVIEW

---

The goal of this thesis work is to optimize the neutron transport step of a coupled, multi-physics process occurring in a system that has moving components. One important application of this work is the quantification of the shutdown dose rate (SDR) during maintenance operations in fusion energy systems (FES).

During the operation of a fusion device, the nuclear reactions (e.g. D-T fusion) occurring in the plasma result in the production of high energy (14 MeV) neutrons that penetrate deeply into the system components. Some of the neutron reaction pathways result in the production of radioisotopes that persist long after device shutdown. The activated components emit high energy photons as they reach stability over time. These high energy photons can cause grave health effects, therefore it is necessary to quantify the dose rate in order to ensure the safety of personnel working in fusion facilities. This is not only important for the time during operation and immediately after shutdown when the device is in a static configuration, but quantifying the dose rate during a maintenance activity when activated components are moving around the facility.

Performing computational simulations of the radiation transport in these devices and calculating quantities of interest, such as flux and dose rate, are a crucial part of the fusion reactor design phase. These simulations can inform decisions about sustainability and safety of the device. This chapter will provide background on computational radiation transport, methods for SDR analysis, methods for optimizing radiation transport calculations, and finally how radiation transport calculations are currently handled in systems with moving geometries and sources.

## 2.1 Analog Monte Carlo Calculations

The quantification of the SDR requires a detailed distribution of the neutron and photon flux throughout all regions of phase space (space, energy, and direction). Due to the size and complexity of FES, the most optimal way to obtain accurate particle distributions is through Monte Carlo (MC) radiation transport rather than deterministic methods.

In general, MC calculations rely on repeated random sampling to solve mathematical problems. In radiation transport applications, the MC method is used to solve the Boltzmann transport equation [12] through the simulation of random particle walks through phase space. In analog operation mode (i.e. no variance reduction), the source particle's position, energy, direction and subsequent collisions are sampled from probability distribution functions (PDFs). Quantities of interest such as flux can be scored, or tallied, by averaging particle behavior in discrete regions of phase space.

do I mention deterministic anywhere else?

One challenge incurred by MC simulations of FES is the presence of heavily shielded regions. The particles undergo a high degree of collisions (absorption and scattering) in the shielding which results in low particle fluxes in the attenuated regions. Regions that have low particle fluxes have higher statistical uncertainty.

The statistical error is a function of the relative error,  $\mathfrak{R}$ , which is defined as

$$\mathfrak{R} = \frac{\sigma_{\bar{x}}}{\bar{x}} \quad (2.1)$$

where  $\bar{x}$  is the average of the tally scores, and  $\sigma_{\bar{x}}$  is the standard deviation of the tally scores. For a well behaved tally,  $\mathfrak{R}$  is proportional to  $1/\sqrt{N}$  where  $N$  is the number of tally scores [3].

The relative error is inversely proportional to the number of tally scores. Therefore, to reliably predict results in these regions, many particle histories need to be simulated which can require large amounts of computer

time.

The efficiency of MC calculations is measured by a quantity known as the figure of merit (FOM). The FOM is a function of relative error,  $\mathfrak{R}$ , and computer processing time,  $t_{\text{proc}}$ , as given by

$$\text{FOM} = \frac{1}{\mathfrak{R}^2 t_{\text{proc}}} \quad (2.2)$$

A high FOM is desirable because it means that less computation time is needed to achieve a reasonably low error ( $>0.1$  [3]).

## 2.2 Shutdown Dose Rate Analysis

This section will discuss the two primary workflows used to investigate the SDR: the Direct 1-Step (D1S) [4] and the Rigorous 2-Step (R2S) [6] method. Both methods couple the neutron and photon transport via activation analysis to calculate the SDR.

### 2.2.1 D1S

As its name implies, the D1S method performs coupled neutron-photon transport in the same simulation. It relies upon a modified version of the MC code, MCNP5, with special cross-section data and the FISPACT nuclear inventory code for time correction factors. The nuclear data available in the standard MCNP code includes prompt photon production cross sections,  $\sigma_{n,\gamma}$ . If a prompt photon reaction is sampled, the photon is stored until the original neutron transport is completed. Then, the photon is transported as part of the same simulation. The version of MCNP5 used by D1S includes a set of modified cross sections that approximate the transmutation process. This allows the delayed photons to be emitted as prompt so they can be transported in the same simulations as neutrons. A time correction factor is later applied. Because both neutron and photon transport occur in the

same simulation, therefore on the same geometry, D1S is not currently applicable to geometries that undergo movement after shutdown. This has been identified as a necessary improvement and the development of a subroutine to produce portable decay photon sources for pure photon calculations is underway [5].

### 2.2.2 R2S

In contrast to D1S, the R2S method relies upon separate MC neutron and photon transport simulations. The transport steps are coupled through activation analysis by a dedicated nuclear inventory code. The goal of the neutron transport step is to determine the neutron flux as a function of space and energy. This neutron flux along with a specific irradiation and decay scenario are used as input into a nuclear inventory code to determine the photon emission density as a function of decay time. The calculated photon emission density for each decay time is then used as the source for MC photon transport. A photon flux tally fitted with flux-to-dose-rate conversion factors is used to determine the final SDR [6].

## 2.3 Monte Carlo Variance Reduction Methods

As mentioned in section 2.1, the presence of heavy shielding in FES presents a challenge for MC calculations because of the high degree of uncertainty caused by low particle fluxes. A set of techniques, known as variance reduction (VR), improve the efficiency of these calculations by reducing the compute time necessary to achieve a statistically reasonable result.

More specifically, VR methods aim to increase the FOM given in Eq. 2.2 by increasing  $N$  and decreasing  $\mathfrak{R}$ , a function of  $\sigma_{\bar{x}}$ , by preferentially sampling trajectories that are likely to contribute to the tallies of interest.

One way this is accomplished is by sampling from biased PDFs that govern particle behavior. In order to compensate for this biased sampling, the particle statistical weight is adjusted accordingly [1]. The relationship between the particle statistical weight,  $w$ , and the PDF that governs particle behavior is as follows

$$w_{\text{biased}} \text{pdf}_{\text{biased}} = w_{\text{unbiased}} \text{pdf}_{\text{unbiased}} \quad (2.3)$$

If this biased sampling results in an event occurring more frequently than it actually does, the particle weight is decreased and vice versa.

One of the earliest and still commonly used methods of VR is particle splitting and rouletting. This is particularly useful in simulations where particles penetrate deeply into shielded regions, like in FES. To increase the number of particle histories that can contribute to a tally of interest, it is desirable to split particles as they enter more important regions and roulette particles as they enter less important regions. The decision to split or roulette particles first requires assigning an importance,  $I$ , to every region in the geometry. When a particle moves from a region A to a region B, the ratio of importances is calculated. If region B is more important than region A such that  $I_B/I_A \geq 1$ , the particle with original weight  $w_0$  is split into  $N = I_B/I_A$  particles, each with weight  $w_0/N$ . If instead region B is less important than region A such that  $I_B/I_A < 1$ , the particle will undergo roulette. The particle will survive with a probability  $N$  and weight  $w_0/N$  [2].

The weight window method in the Monte Carlo N-Particle (MCNP) code utilizes both splitting and rouletting. A weight window is a region of phase-space that is assigned an upper and lower bound. The windows can be assigned to cells in the geometry, on a superimposed mesh, and to energy bins. When a particle enters a weight window, its weight is assessed; if its weight is above the upper bound, it is split and if it is below the lower bound, it is rouletted. There are various methods to produce

these weight window bounds automatically which drastically reduces the time, effort, and expertise required by the analyst. Some of these methods will be discussed in the following section.

## 2.4 Automated Variance Reduction

Historically, VR techniques have required a priori knowledge of the problem physics in order to assign importance parameters. Many techniques have been developed over the years to automate the selection and assignment of these parameters to reduce computational and human effort.

One class of VR techniques, known as hybrid deterministic/MC methods, is based upon the solution to the adjoint Boltzmann transport equation having significance as the measure of importance of a particle to some specified objective function. Because deterministic solutions to the transport equation require much less computation time, they are useful as an estimate of the adjoint particle flux throughout phase space. To demonstrate the use of the adjoint solution as an importance function, first start with the operator form of the linear, time-independent Boltzmann transport equation [12]

$$H\Psi(\vec{r}, E, \hat{\Omega}) = q(\vec{r}, E, \hat{\Omega}) \quad (2.4)$$

where  $\Psi$  is the angular flux,  $q$  is the source of particles, and the operator  $H$  which describes all particle behavior is given by

$$H = \hat{\Omega} \cdot \nabla + \sigma_t(\vec{r}, E) - \int_0^\infty dE' \int_{4\pi} d\Omega' \sigma_s(\vec{r}, E' \rightarrow E, \hat{\Omega}' \rightarrow \hat{\Omega}) \quad (2.5)$$

where  $\sigma_t$  is the total cross-section and  $\sigma_s$  is the double-differential scattering cross-section. The source and angular flux are functions of five independent variables: a three-dimensional position vector ( $\vec{r}$ ) a two-dimensional directional vector ( $\hat{\Omega}$ ), and energy ( $E$ ). The adjoint identity is



stated as

$$\langle \Psi^+, H\Psi \rangle = \langle \Psi, H^+\Psi^+ \rangle \quad (2.6)$$

where  $\langle \cdot \rangle$  refers to the integration over space, energy, and angle and the adjoint operator  $H^+$  is given by

$$H^+ = -\hat{\Omega} \cdot \nabla + \sigma_t(\vec{r}, E) - \int_0^\infty dE' \int_{4\pi} d\Omega' \sigma_s(\vec{r}, E \rightarrow E', \hat{\Omega} \rightarrow \hat{\Omega}') \quad (2.7)$$

This identity can be used to form the adjoint transport equation.

$$H^+\Psi^+ = q^+ \quad (2.8)$$

Substituting Eq.2.5 and 2.8 into Eq. 2.6, the adjoint identity can also be written as

$$\langle \Psi^+, q \rangle = \langle \Psi, q^+ \rangle \quad (2.9)$$

As mentioned, the solution to the adjoint transport equation will be used as an importance function therefore the thoughtful selection of an adjoint source  $q^+$  is needed.

Consider the equation for detector response,  $R$

$$R = \langle \Psi, \sigma_d \rangle \quad (2.10)$$

where  $\sigma_d$  is a detector response function. If the adjoint source is chosen to be equivalent to the detector response function,

$$q^+ = \sigma_d \quad (2.11)$$

and substituted into Eq. 2.10

$$R = \langle \Psi, q^+ \rangle \quad (2.12)$$

the response has the same form as the right side of Eq. 2.9, therefore the

response can also be written as

$$R = \langle \Psi^+, q \rangle \quad (2.13)$$

This final relation allows us to know the response  $R$  for any source  $q$  once the adjoint flux  $\Psi^+$  for a detector of interest is known.

### 2.4.1 CADIS

The Consistent Adjoint Driven Importance Sampling (CADIS) method is one of the hybrid deterministic/MC VR techniques that uses the adjoint solution as an importance function to formulate source and transport biasing parameters for MC transport [1]. More specifically, CADIS provides a method for generating a biased source and the weight window lower bounds in a consistent manner. Recall that the response, or tally, of interest in a transport calculation can be represented in terms of the adjoint flux by Eq. 2.13. To decrease the variance, the CADIS method formulates a biased source distribution that represents the contribution of particles from phase space  $(\vec{r}, E, \hat{\Omega})$  to the total detector response,  $R$ .

$$\hat{q}(\vec{r}, E, \hat{\Omega}) = \frac{\Psi^+(\vec{r}, E, \hat{\Omega}) q(\vec{r}, E, \hat{\Omega})}{R} \quad (2.14)$$

This essentially is a way to bias the sampling of source particles as a function of their contribution to the total detector response. As previously mentioned, when sampling from a biased distribution, the particle weight needs to be adjusted to eliminate systematic bias.

$$w(\vec{r}, E, \hat{\Omega}) \hat{q}(\vec{r}, E, \hat{\Omega}) = w_0 q(\vec{r}, E, \hat{\Omega}) \quad (2.15)$$

Substituting in Eq. 2.14 and setting  $w_0$  equal to one, the corrected particle weight is given as

$$w(\vec{r}, E, \hat{\Omega}) = \frac{R}{\Psi^+(\vec{r}, E, \hat{\Omega})} \quad (2.16)$$

There is an inverse relation to the adjoint flux, or importance function. This relationship for the particle statistical weight is used in the source sampling and transport process so that source particles are created with weights that reside within their corresponding weight window. The equation for weight window lower bounds is given as

$$w_l(\vec{r}, E, \hat{\Omega}) = \frac{R}{\Psi^+(\vec{r}, E, \hat{\Omega})^{(\frac{\alpha+1}{2})}} \quad (2.17)$$

The width of the weight windows is determined by a parameter defined to be the ratio between upper and lower bounds  $\alpha = w_u/w_l$ . MCNP uses a default value of 5 for  $\alpha$ .

CADIS is ideally suited to reduce the variance of a detector response in a single target. There are other methods, such as FW-CADIS, that are suited for reducing the variance in several targets or even globally.

## 2.4.2 FW-CADIS

The Forward-Weighted CADIS method is another hybrid deterministic/MC VR method. FW-CADIS aims to increase the efficiency of detector responses globally or in multiple localized targets [7]. The goal is to create uniform particle density in the tally regions so in turn, there is uniform statistical uncertainty in the MC solution. This method relies upon a forward deterministic transport solution to weight the source for adjoint deterministic transport. The adjoint solution is then used with the standard CADIS method to produce source and transport biasing parameters for the forward MC transport simulation.

If the objective is a spatially dependent total response rate, the FW-

CADIS adjoint source is formulated as

$$q^+(\vec{r}, E) = \frac{\sigma_d(\vec{r}, E)}{\int_E \phi(\vec{r}, E) \sigma_d(\vec{r}, E) dE} \quad (2.18)$$

where  $\sigma_d(\vec{r}, E)$  is the response function. This effectively weights the adjoint source by the inverse of the total forward response which means that in regions with low forward flux, the adjoint flux, and therefore importance, will be high and vice versa. This will result in the overall goal of nearly equal statistical uncertainty in regions of interest.

## 2.5 Automated Variance Reduction for Multiphysics

In its essence, SDR analysis is the analysis of a coupled, multiphysics system; the initial neutron irradiation is coupled to the decay photon transport through activation analysis. As discussed in section 2.2.2, the R2S method requires separate MC calculations for the neutron and photon transport. Applying this workflow to full-scale, 3D FES becomes impractical due to the computational effort required to produce accurate space- and energy-dependent fluxes throughout the geometry.

Optimizing the final step, photon transport in the case of SDR analysis, can be done through a straightforward application of the CADIS method to solve for the response at a single detector or the FW-CADIS method if the response is desired in multiple detectors or globally.

Optimizing the initial step of a multi-step process, neutron transport in the case of SDR, is not as straightforward. The Multi-Step CADIS method described in the next section provides an explanation for this challenge and a method for solving it.

### 2.5.1 MS-CADIS

The Multi-Step Consistent Adjoint Weighted Importance Sampling (MS-CADIS) method of variance reduction was developed to optimize the primary radiation transport in a coupled, multi-step process.

Optimizing the initial radiation transport relies upon an importance function that represents the importance of the particles to the final response of interest, not the response of that individual step [8]. This is challenging because the the final response of interest depends on the subsequent steps of the multi-step process.

MS-CADIS can be applied to any coupled, multi-step process, but when applied to SDR calculations, it aims to increase the efficiency of the neutron transport step using an importance function that captures the potential of regions to become activated and the importance of the resulting decay photons to the final SDR [8].

The detector response can be expressed as the integral of the importance function,  $I$ , multiplied by the source distribution,  $q$

$$R = \langle I(\vec{r}, E), q(\vec{r}, E) \rangle \quad (2.19)$$

MS-CADIS provides a method to calculate an approximation of this importance function where the response is the final response of the multi-step process. In the case of an R2S calculation, the final response is the SDR caused by the decay photons. The SDR is defined as

$$SDR = \langle \sigma_d(\vec{r}, E_\gamma), \phi_\gamma(\vec{r}, E_\gamma) \rangle \quad (2.20)$$

where  $\sigma_d$  is the flux-to-dose-rate conversion factor at the position of the detector and  $\phi_\gamma$  is photon flux. If the adjoint photon source is chosen to be  $\sigma_d$ , the importance function,  $I$ , is defined as the adjoint solution,  $\phi_\gamma^+$

leading to the following relationship

$$\text{SDR} = \langle q_\gamma^+(\vec{r}, E_\gamma), \phi_\gamma(\vec{r}, E_\gamma) \rangle = \langle q_\gamma(\vec{r}, E_\gamma), \phi_\gamma^+(\vec{r}, E_\gamma) \rangle \quad (2.21)$$

Because the final goal is an importance function that represents the importance of neutrons the final SDR, the neutron adjoint identity is also set equal to the photon response.

$$\text{SDR} = \langle q_n^+(\vec{r}, E_n), \phi_n(\vec{r}, E_n) \rangle = \langle q_n(\vec{r}, E_n), \phi_n^+(\vec{r}, E_n) \rangle \quad (2.22)$$

Combining equations 2.21 and 2.22, gives the relationship between the neutron and photon responses.

$$\langle q_n^+(\vec{r}, E_n), \phi_n(\vec{r}, E_n) \rangle = \langle q_\gamma(\vec{r}, E_\gamma), \phi_\gamma^+(\vec{r}, E_\gamma) \rangle \quad (2.23)$$

In order to use the adjoint neutron flux as an importance function to optimize the neutron transport, a solution for the adjoint neutron source,  $q_n^+$ , is needed. This requires an equation relating the photon source,  $q_\gamma$ , to the neutron flux,  $\phi_n$ .

## 2.5.2 GT-CADIS

The Groupwise Transmutation (GT)-CADIS method, an implementation of MS-CADIS solely for SDR analysis, provides a solution to the adjoint neutron source by calculating a coupling term that relates the neutron flux to the photon source [11].

The decay photon source at a single point can be expressed as this non-linear function of  $\phi_n$

$$q_\gamma(E_\gamma) = \int_{E_n} f(\phi_n) dE_n \quad (2.24)$$

This function can not be linearized for arbitrary transmutation networks

and irradiation scenarios, but a linear relationship can be formulated when a set of criteria, known as the Single Neutron Interaction Low Burnup (SNILB) criteria, are met. The SNILB criteria can be used to obtain solutions for the coupling term,  $T(\vec{r}, E_n, E_\gamma)$ , which is defined by the following equation.

$$q_\gamma(\vec{r}, E_\gamma) = \int_{E_n} T(\vec{r}, E_n, E_\gamma) \phi_n(\vec{r}, E_n) dE_n \quad (2.25)$$

If a  $T$  can be found that satisfies this relationship, Eq. 2.25 can be substituted into the photon source in Eq. 2.23 which can be used to solve for the adjoint neutron source given below

$$q_n^+(\vec{r}, E_n) = \int_{E_p} T(\vec{r}, E_n, E_p) \phi_p^+(\vec{r}, E_p) dE_p \quad (2.26)$$

To calculate  $T$ , A series of single energy group neutron irradiations is performed on each material in the geometry. This results in a photon source that is a function of each neutron energy group. According to Eq. 2.25, dividing this photon source by the neutron flux results in the coupling term  $T$ .

It has been shown that for typical FES spectra, materials, and irradiation scenarios, the SNILB criteria are met; therefore, GT-CADIS provides a solution for  $T$ , and therefore the adjoint neutron source needed to optimize the neutron transport for SDR analysis of FES.

## 2.6 Moving Geometries and Sources

### 2.6.1 MCNP6 Moving Objects Capability

Historically, Monte Carlo analysis of dynamic systems was performed using a series of separate simulations with different input files that contained step-wise changes of the geometry configuration. The new moving object capability that will be available in a future version of MCNP6 allows

for the motion of objects, sources, and delayed particles during a single simulation [9], [10]. This capability allows for rigid body transformations of objects including rectilinear translations and curvilinear translations and rotations. The objects can move with constant velocity, constant acceleration, or be relocated. Object kinetics are not treated so the user must use caution and supply transformations that will not cause objects to overlap. This capability is currently applicable to MCNP's native geometry format, constructive solid geometry (CSG), and is not available for mesh-based geometries.

Sources can be assigned to moving objects, therefore can move with the same dynamics as other objects in the problem. This capability also allows for the treatment of secondary particles emitted by objects in motion. This treatment is only approximate because the geometry is fixed during the transport of source or delayed particles. This is a valid approximation due to the assumption that the geometry movement is orders of magnitude slower than particle transport.

During the MCNP simulation, source particles are tracked through the geometry from the time of emission to termination. If any of the source particle's interactions result in the creation of a prompt or delayed secondary particle, that information is stored. After the source particle has terminated, any stored secondary particles are retrieved and transported. In the case of delayed particles emitted from moving objects, the location, direction, energy, and time are stored at the time of fission or activation and then at the time of emission, the geometry configuration is updated to provide the correct location and orientation of the delayed particle at the time of emission.

## **2.6.2 MCR2S with Geometry Movement**

The Mesh Coupled implementation of R2S (MCR2S), developed by the Culham Science Center, was updated to allow geometry components to



change location after shutdown [13]. This capability was developed to facilitate SDR calculation during maintenance and intervention activities. MCR2S relies on MCNP for both neutron and photon transport steps and FISPACT for the activation calculations. It allows multiple components to be moved to different locations prior to the photon transport step.

These geometry translations occur by creating a copy of the components that will move. Transform cards are applied to the copies. The original components remain in their original locations and their material is changed to vacuum. Any source particle that starts in one of the components that moves after shutdown is automatically translated to the correct location.

The requirement that both the original component (set as void) and its transformed copy are present during the photon transport step means that there can be no overlap between the parts which could be problematic for small transformations.

## 3 EXPERIMENT

---

### 3.1 Demonstration of GT-CADIS

GT-CADIS has proven to be an effective method for optimizing the neutron transport step of SDR analysis in static FES where the SNILB criteria are met. As it stands, this method will not provide appropriate VR parameters for the cases where activated components are moving after shutdown. The following experiment will demonstrate the need for a time-integrated adjoint photon solution in order to provide useful VR parameters for dynamic systems.

#### 3.1.1 Problem Description

The geometry chosen for this demonstration is a simplified representation of a fusion energy device shown in Fig. 3.1. It is composed of a chamber of Stainless Steel 316 (SS-316) with a central cavity measuring 2m x 2m x 2 m. The walls are 2 m thick. The chamber is surrounded by air and there is helium in the central cavity. A CAD model of this geometry was created and tagged with Trelis [?]. A spatially uniform source of 13.8-14.2 MeV neutrons was placed in the central cavity. The SDR is measured with a detector after a single pulse irradiation of  $10^5$  s and decay period of  $10^5$  s. The detector is a sphere, 10 cm in radius, located 2 m outside of the steel chamber in the x-direction. The detector material was chosen to be the same as that used in a previous GT-CADIS experiment (52.34 at. % H-1, 47.66 at. % C-12) [11].

First, the R2S workflow was performed with analog (except for implicit capture) MC neutron and photon transport steps. Then, the GT-CADIS method was used to generate VR parameters to optimize the neutron transport step.



Figure 3.1: Planar view of the geometry. Steel chamber with 2 m thick and central cavity measuring 2 m x 2 m x 2 m. The central cavity is filled with helium and chamber is surrounded by air. A SDR detector is located 2 m in the x-direction from the chamber.

### 3.1.2 Analog R2S

The main steps of the R2S workflow are as follows:

1. MC Neutron Transport
2. Activation Analysis
3. MC Photon Transport

MCNP5 [?] was chosen as the MC code and ALARA [?] as the activation code.

First, a DAGMCNP5 [15] simulation with  $10^7$  histories was run using the CAD geometry generated by Trelis and an input file that contained a Cartesian mesh flux tally over the entire geometry. The neutron flux tally was binned into the 175 group VITAMIN-J energy structure [?]. The

resulting neutron flux and relative error for the 13.8-14.2 MeV energy group is shown in Fig. 3.2.

The Python for Nuclear Engineering (PyNE) toolkit has many useful functions and scripts to assist in nuclear analysis [?]. One script in the PyNE toolkit's R2S module was used to construct the ALARA input files using the neutron flux mesh. ALARA was run using FENDL2.0 nuclear data [?]. PyNE R2S was used again to generate a mesh-based photon source from the ALARA output. The photon source is shown in Fig. 3.3.

### 3.1.3 GT-CADIS

After the the R2S workflow was carried out with analog MC transport, the GT-CADIS method was used to generate a biased source and weight windows to optimize the neutron transport step. The main steps of the GT-CADIS method are as follows:

1. Deterministic adjoint photon transport
2. Calculation of the GT-CADIS adjoint neutron source
3. Deterministic adjoint neutron transport
4. Generation of biased source and weight windows from adjoint neutron flux

The deterministic code PARTISN [14] was chosen to perform the adjoint transport steps. The source used for adjoint photon transport was a 42 energy group VITAMIN-J discretization of the ICRP-74 flux-to-dose conversion factors [16]. The CAD geometry was discretized onto a conformal Cartesian mesh. The resulting adjoint photon flux mesh is shown in Fig. 3.4.

Next, the coupling term  $T$  is calculated for each material: SS316, air, and helium. This is done by performing separate  $1E5$  s irradiation and

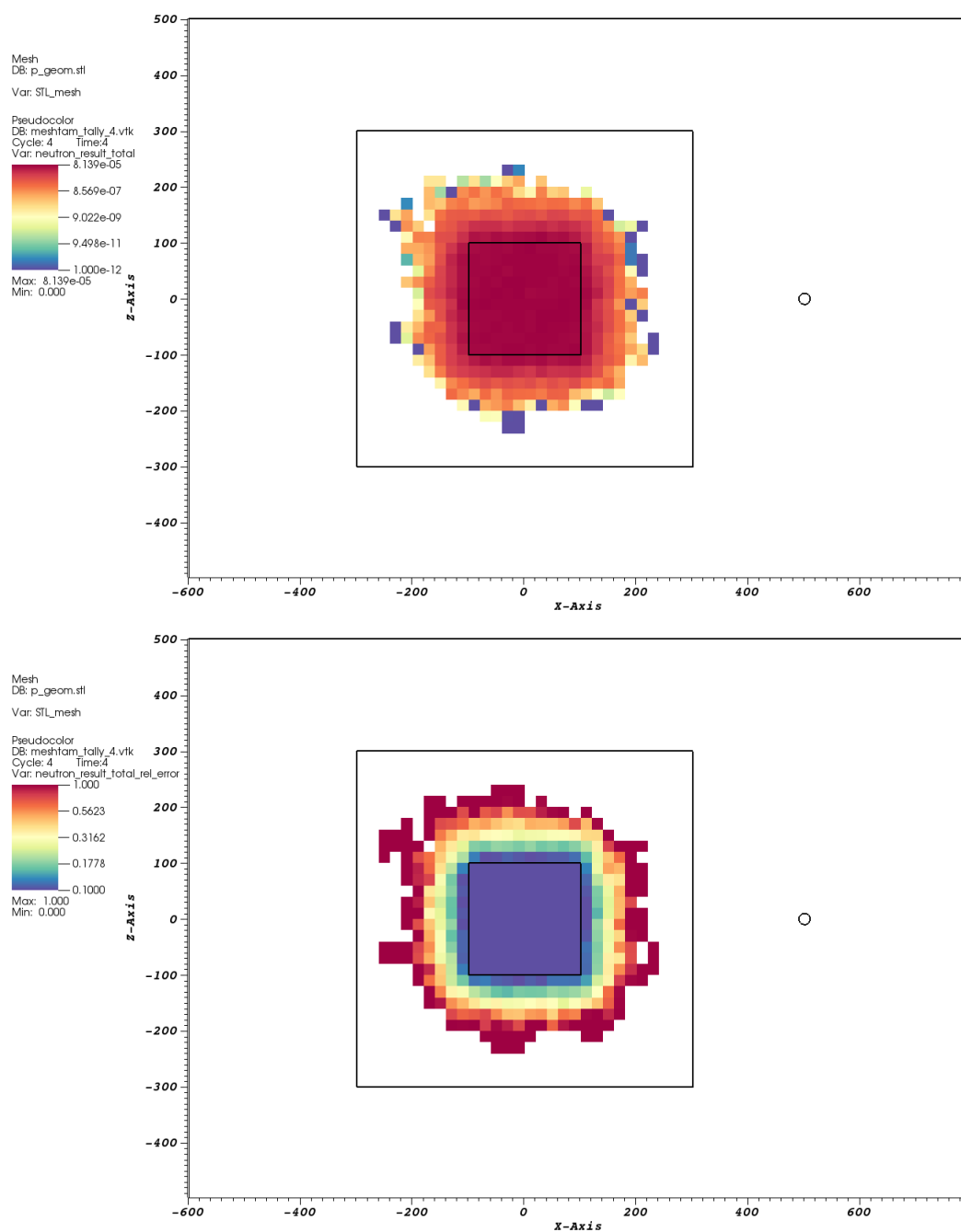


Figure 3.2: Neutron flux and relative error resulting from analog MC simulation.

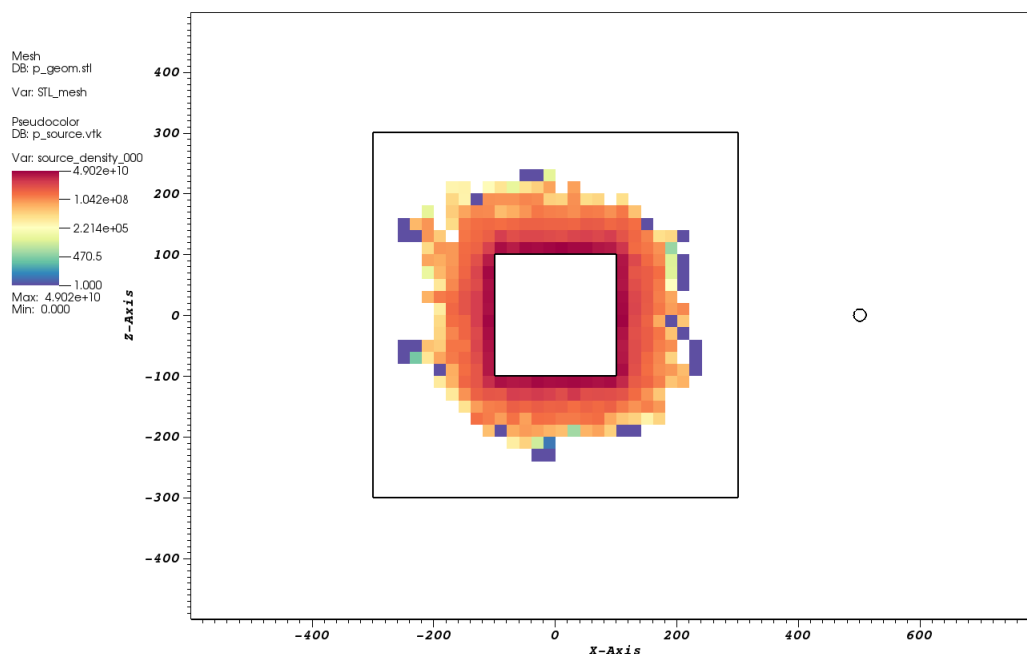


Figure 3.3: Photon source generated after ALARA activation calculation using the analog MC neutron transport result.

1E5 s decay ALARA simulations for each of 175 neutron groups in each of the materials to obtain the photon source in each photon energy group as a function of the neutron flux in each neutron energy group. T was then calculated using Eq. 2.25.

This T is combined with the adjoint photon flux to generate the GT-CADIS adjoint neutron source via Eq. 2.26. PARTISN is run again using this adjoint neutron source and the resulting adjoint neutron flux for the 13.8-14.2 MeV is shown in Fig. 3.5.

This adjoint neutron flux functions as an importance map of neutrons to the final SDR. In the region of the steel chamber near the detector, there is a high flux, therefore neutrons in this region have a high importance to the SDR. In contrast, there is a low flux in the regions on the far side of the detector. Neutrons in this region are not as important to the SDR.

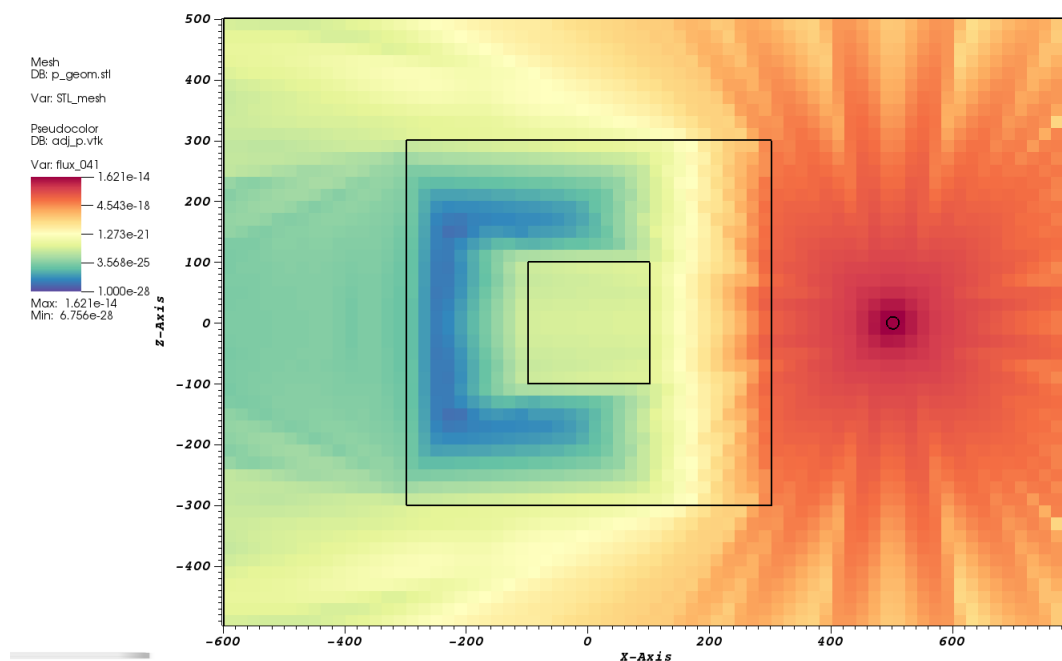


Figure 3.4: Adjoint photon flux used to generate adjoint neutron source.

The adjoint neutron flux is used to generate the biased source and weight windows via the CADIS method. These are seen in Fig. 3.6 and Fig. 3.7.

The biased source and weight window files were used to optimize the neutron transport step of R2S. A DAGMCNP5 simulation with  $10^7$  histories was performed using these VR parameters and the resulting neutron flux and relative error are shown in Fig. 3.8.

ALARA was run using the neutron flux and the same irradiation and decay scenario used to calculate T. The photon source distribution generated is shown in Fig. 3.9

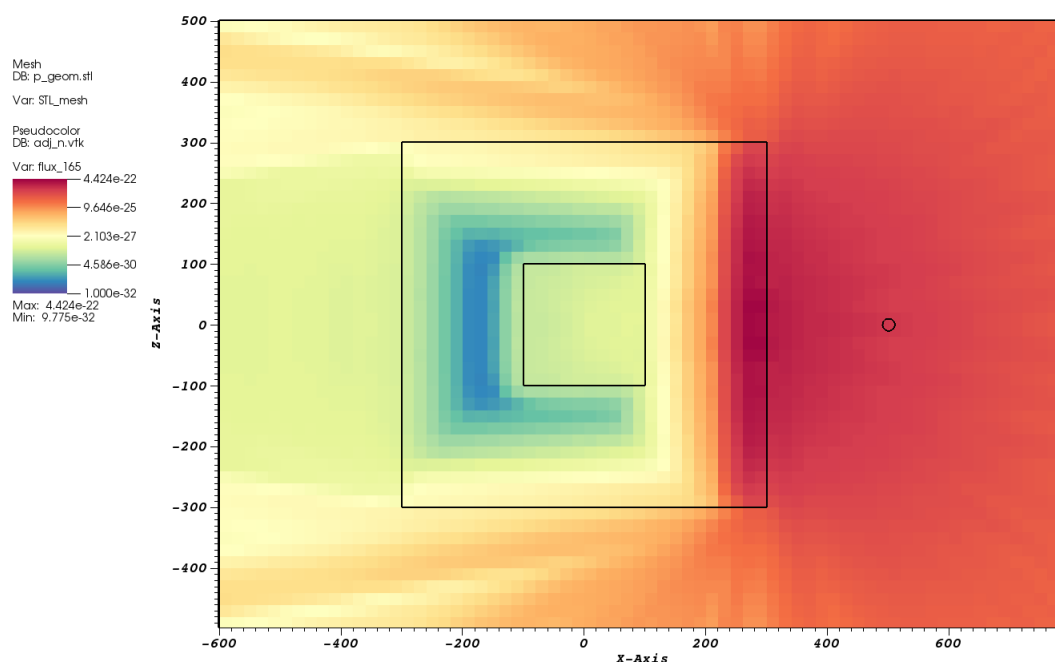


Figure 3.5: Adjoint neutron flux used to generate the biased source and weight windows.

## 3.2 Limitations of GT-CADIS for Moving Systems

Comparing the neutron flux and relative error obtained by the analog MC transport ?? and that obtained using the GT-CADIS method 3.8, it is clear to see that given the same number of histories, the GT-CADIS method not only reduces the error in regions of the steel chamber that are important to the SDR, but allows a solution to be calculated in the detector region.

Now, consider if the steel chamber was not a monolithic block, and instead made of modular components that move after shutdown, during the photon decay process.

For example, a component of the chamber located on the far side of the



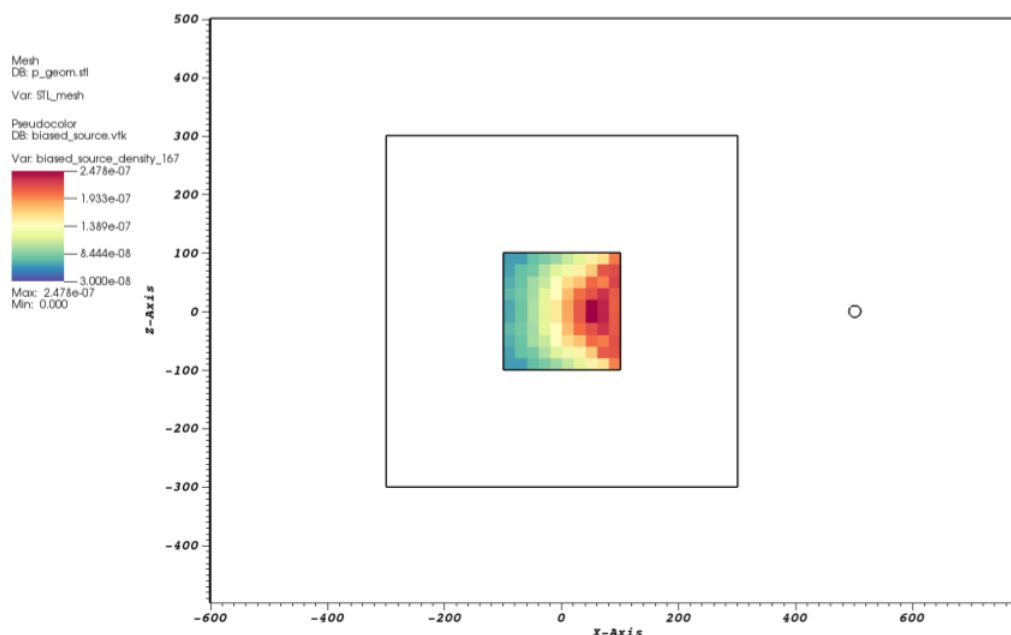


Figure 3.6: Biased neutron source generated with GT-CADIS method.

detector moving to a location near the detector as shown in Fig. 3.10. The photons produced in that component now become important to the SDR at the detector. This also means that the neutrons in this region are important because it is the neutron irradiation that results in photon emission.

Highlighting the region of the moving component in the adjoint neutron flux produced by GT-CADIS, Fig. 3.11, it can be seen that this is no longer a valid importance map of the neutrons to the final SDR. There is a low flux, therefore low importance in the moving component that will eventually be positioned near the detector. Because this adjoint neutron flux is used to generate source and transport biasing parameters, neutrons will be steered away from interactions in this component, increasing the uncertainty in a region that will ultimately be important to the SDR.

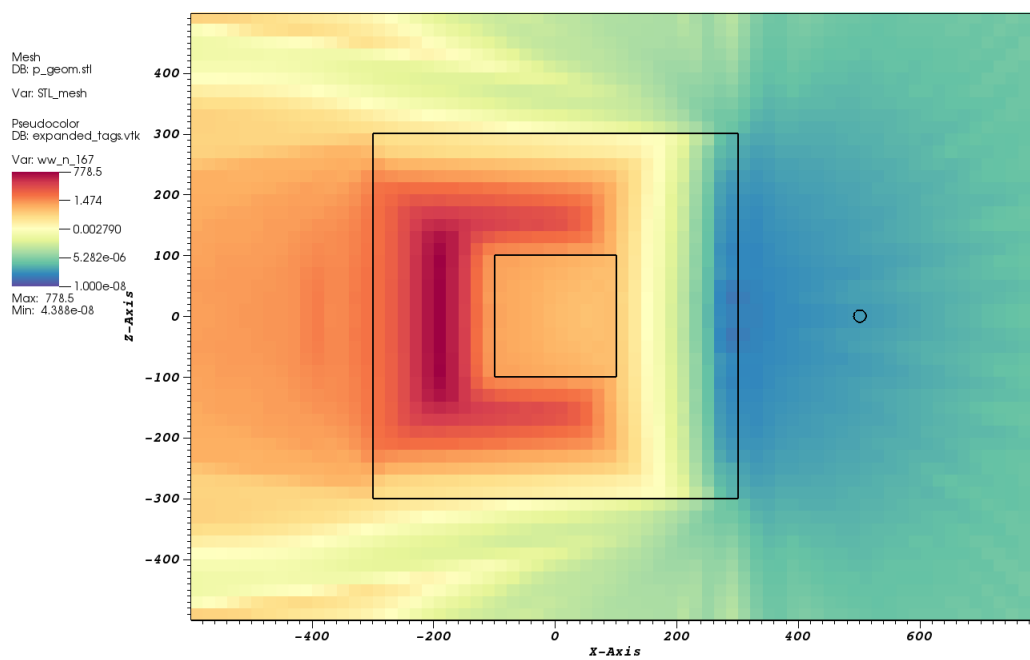


Figure 3.7: Weight window mesh generated with GT-CADIS method.

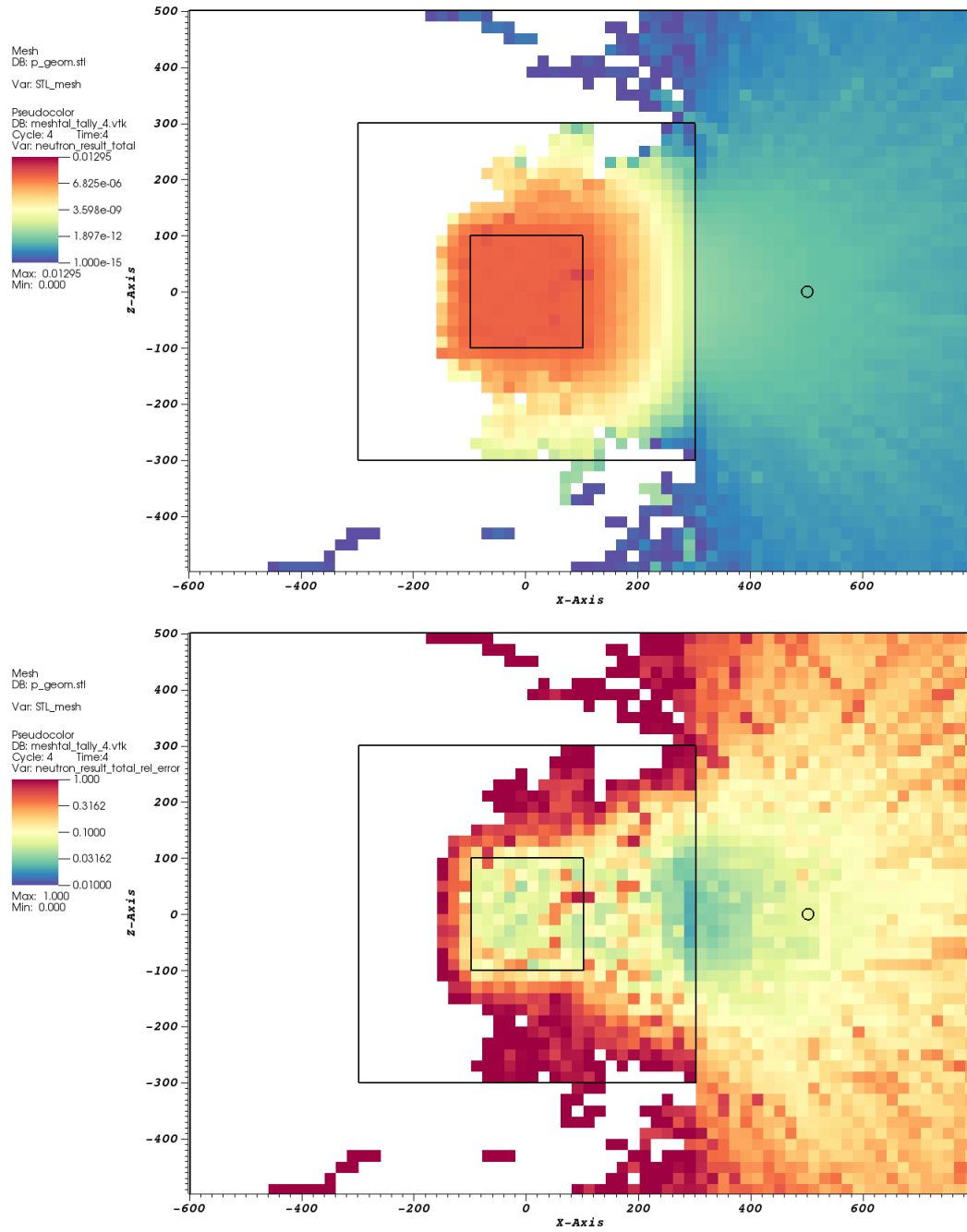


Figure 3.8: Neutron flux and relative error resulting from MC simulation using GT-CADIS biased source and weight window mesh.

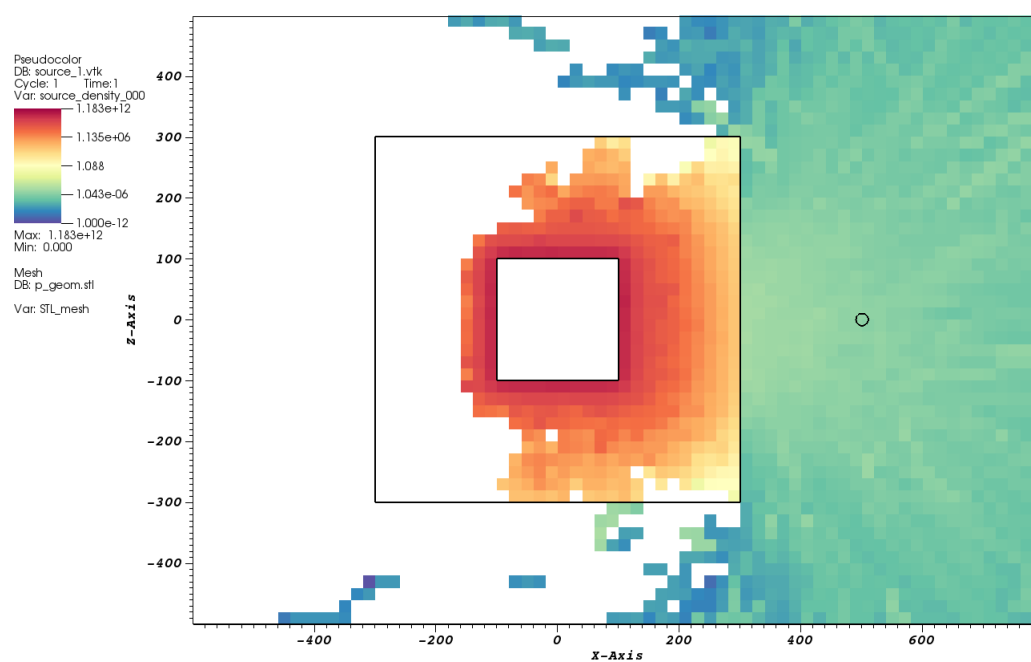


Figure 3.9: Photon source generated after ALARA activation calculation using the GT-CADIS optimized neutron transport result.

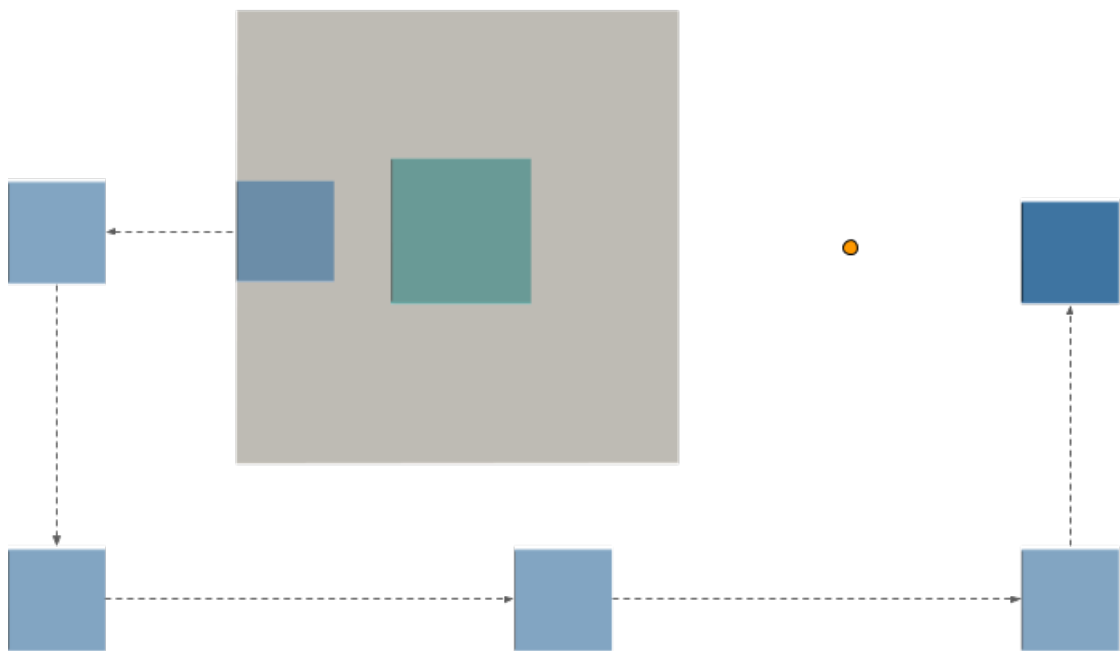


Figure 3.10: Path of activated component moving from the far side of the SDR detector to position next to it.

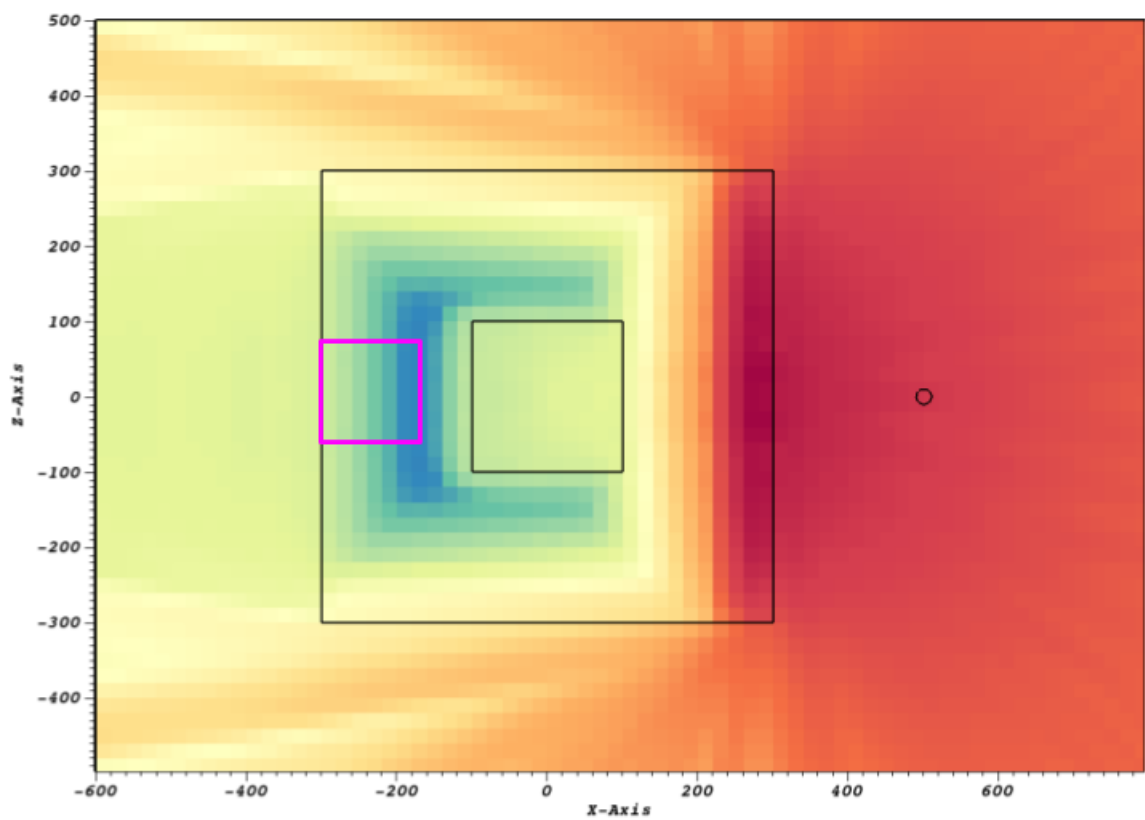


Figure 3.11: Adjoint neutron flux, highlighted region of moving component

## 4 VARIANCE REDUCTION FOR TIME-INTEGRATED MULTIPHYSICS ANALYSIS

---

The Multi-Step Consistent Adjoint Weighted Importance Sampling (MS-CADIS) method of variance reduction was developed to optimize the primary radiation transport in a coupled, multi-step process. The first implementation of this method was applied to the coupled neutron activation-photon decay process that occurs in FES. In its current form, MS-CADIS is only applicable to static systems where the geometry remains unchanged in all steps of the multi-step process.

This chapter will first discuss MS-CADIS outside of the context of SDR analysis. Next, a time-integrated solution to the adjoint of the physical process occurring during geometry movement will be derived. Finally, this time-integrated solution will be applied to the GT-CADIS method to form the TGT-CADIS adjoint neutron source that will optimize the neutron transport step of SDR analysis.

### 4.1 Generalized MS-CADIS Method

In the current literature, MS-CADIS is primarily discussed as it applies to SDR analysis [8]. In actuality, MS-CADIS can be applied to any multi-step process in which the primary radiation transport is coupled to a secondary physical process. The addition of time integration to this methodology can also be applied to any coupled multiphysics process. For this reason, it is prudent to discuss MS-CADIS in a more generalized manner.

To describe the system of coupled, multiphysics, the operator notation of the Boltzmann transport equation

$$H\phi = q \tag{4.1}$$

where  $H$  operates on the particle flux  $\phi$  and  $q$  is a source of particles, will be used to represent the initial radiation transport and an equation of the same form

$$L\Psi = b \quad (4.2)$$

where  $L$  operates on some function  $\Psi$  and  $b$  is a source term, will be used to describe a generic secondary physics. The adjoint identity for the neutral particle transport equation was given in Eq. 2.9. This identity is valid for an arbitrary adjoint source function [12], therefore the secondary physics has an adjoint identity of the same form

$$\begin{aligned} \langle \Psi^+, L\Psi \rangle &= \langle \Psi, L^+\Psi^+ \rangle \\ \langle \Psi^+, b \rangle &= \langle \Psi, b^+ \rangle \end{aligned} \quad (4.3)$$

where  $\langle \cdot \rangle$  signifies the integration over all dependent variables. This is a two-step system, therefore the response of the secondary physics is the final response of interest and takes the form

$$R_{\text{final}} = \langle \sigma_b, \Psi \rangle \quad (4.4)$$

According to the CADIS method, if the adjoint source is set equal to the detector response function, the adjoint solution forms the importance function. Substituting  $b^+$  into Eq. 4.4 yields the following

$$R_{\text{final}} = \langle \Psi, b^+ \rangle \quad (4.5)$$

Combining Eq. 4.5 with the adjoint identity yields

$$R_{\text{final}} = \langle \Psi^+, b \rangle \quad (4.6)$$

For a coupled, multi-step process, the MS-CADIS method constrains the primary adjoint response such that it is equal to the final response of



the system as shown below

$$R_{\text{final}} = \langle \phi, q^+ \rangle = \langle \phi^+, q \rangle \quad (4.7)$$

Ultimately, the goal is to find a solution to the adjoint primary radiation transport to use as an importance function for the forward calculation. Therefore, a source for the adjoint radiation transport is needed. Equating the adjoint response equations in Eq. 4.7 and 4.6, yields the expression in Eq. 4.8.

$$\langle \phi, q^+ \rangle = \langle \Psi^+, b \rangle \quad (4.8)$$

In a practical scenario, the forward source of primary physics (e.g. neutron source resulting from D-T fusion) will be known. The adjoint source of secondary physics is chosen to be the response function for the detector of interest (e.g. flux-to-dose conversion factors). Given that these sources are known, both solutions,  $\phi$  and  $\Psi^+$  can be found through transport operations. The source of the forward secondary,  $b$ , and adjoint primary physics,  $q^+$ , are both unknown, therefore a second equation is needed. This is a coupled, multiphysics system where the source of the secondary physics is a response of the primary radiation transport therefore the two processes can be related by the following definition

$$b = \langle \sigma_c, \phi \rangle \quad (4.9)$$

where  $\sigma_c$  is a function that couples the primary radiation transport to the secondary physics.

Consider the process of neutron-induced prompt photon production. In this case, the function,  $\sigma_c$ , is the neutron-gamma production cross section  $\sigma_{n,\gamma}$ . The primary focus of SDR analysis is the process of neutron-induced delayed gamma production. GT-CADIS provides a method for calculating  $\sigma_c$  when certain conditions (known as SNILB) hold true. In

this case, the coupling term,  $T$ , is an approximation of the transmutation process [11]. As long as there is a solution for  $\sigma_c$ , the function that couples the primary and secondary physics together, there also exists a solution for the adjoint radiation transport source. This can be discovered by substituting Eq. 4.9 into Eq. 4.8 and solving for  $q^+$ .

$$q^+ = \langle \sigma_c, \Psi^+ \rangle \quad (4.10)$$

## 4.2 Time-integrated MS-CADIS

If the configuration of the geometry is changing over time during the secondary physics, it will affect the construction of the adjoint radiation transport source,  $q^+$ . The solutions to both forward and adjoint transport will be calculated in discrete volume elements. Instead of a single solution to the adjoint secondary physics, there is a solution at each position and each time.

- $\Psi^+(\vec{r}_v(t), t)$  Adjoint flux in volume element  $v$  at time  $t$
- $\vec{r}_v(t)$  Position of volume element  $v$  at time  $t$

To solve for the adjoint primary source in each volume element,  $q_v^+$ , the time-dependent solutions of the adjoint secondary transport are combined by integrating over time

$$q_v^+ = \int_t \Psi^+(\vec{r}_v(t), t) \sigma_{c,v}(t) dt \quad (4.11)$$

This time-integrated source term is then used for adjoint radiation transport to obtain  $\phi_v^+$ .

### 4.3 Time-integrated GT-CADIS

GT-CADIS is an implementation of MS-CADIS that is specific to SDR analysis. It provides a method to calculate a coupling term,  $T$ , that relates the neutron flux to the photon source.  $T$  is then used to solve for the adjoint neutron source as shown in Eq. 2.26. If the geometry configuration changes after shutdown, the time-integrated MS-CADIS methodology shown in the previous section can be applied to the GT-CADIS adjoint neutron source.

$$q_{n,v}^+(E_n) = \int_t \int_{E_\gamma} T_v(E_n, E_\gamma, t) \phi_\gamma^+(\vec{r}_v(t), E_\gamma, t) dE_\gamma dt \quad (4.12)$$

where  $\phi_\gamma^+(\vec{r}_v(t), E_\gamma, t)$  is the adjoint flux of photons of energy  $E_\gamma$ , in volume element  $v$ , at time  $t$  and  $T_v(E_n, E_\gamma, t)$  is the  $T$  value of the material in volume element  $v$ , at decay time  $t$ .

There is a  $T$  value calculated for every volume element for every decay time of interest. For many practical problems,  $T$  will not change over the course of geometry movement because the time constants of decay and geometry motion are very different. The motion of components occurs over a very short period of time relative to photon decay. Discretizing the energy spectrum into groups, the coupling term that relates the irradiation of the material in volume element  $v$ , by neutrons in energy group  $g$ , to the corresponding source of photons in energy group  $h$ ,  $T_{v,g,h}$ , is found with Eq. 6.2

$$T_{v,g,h} = \frac{q_{\gamma,v,h}(\phi_{n,v,g})}{\phi_{n,v,g}} \quad (4.13)$$

Using this groupwise calculation of  $T$ , the integral in Eq. 4.12 can be

estimated by the sum

$$q_{n,v,g}^+ = \sum_{t_{\text{mov}}} \left( \sum_h T_{v,g,h} \phi_{\gamma,v,h,t_{\text{mov}}}^+ \right) \quad (4.14)$$

where  $t_{\text{mov}}$  is a time step after shutdown that corresponds to a change in geometry configuration and  $\phi_{\gamma,v,h,t_{\text{mov}}}^+$  is the adjoint flux of photons in energy group  $h$ , in volume element  $v$ , at time step  $t_{\text{mov}}$ .

## 5 PROGRESS

---

### 5.1 DAGMC Simulations with Geometry Transformations

This chapter will discuss the progress of 1) a tool to create geometries in different configurations and 2) an update to DAGMCNP that facilitates the implementation of user-supplied geometry transformations. Both are fundamental to this thesis work.

#### 5.1.1 Production of Stepwise Geometry Files

There are various scenarios that involve the motion of geometry components during a radiation transport simulation. One example is the movement of activated components of a fusion energy device during a maintenance operation. A tool has been developed to generate CAD geometry files that capture the movement of components over time.

First, a geometry file of the model in its original position is created. The geometry components are tagged with transformation numbers that correspond to stepwise motion vectors. The tool loads the original geometry and a file containing the motion vectors. The position of the components is updated according to these transformations and a new geometry file is produced for each time step. This tool only handles rigid-body transformations; no geometric deformations or scaling. It also does not handle kinetics, so the user must be cautious to not cause any overlap of components during the motion.

The new geometry files that contain stepwise changes of the geometry configuration are used as the input geometry for transport calculations to determine the response of interest at each time step.

### 5.1.2 DAGMCNP Geometry Transformations

The ability to read transformation (TRn) cards from the MCNP input file and update the position of the geometry has been added to DAGMCNP. This capability relies upon the same tagging of components in the CAD geometry file discussed in the previous section. The transformation will be applied to any geometry component that is tagged with the number on the TR card. If using this capability to perform stepwise radiation transport calculations over time, the user would create one MCNP input file per time step. Each input file should contain the TR cards necessary to update the position of each component to its new location for that time step. During a DAGMCNP simulation, the geometry is loaded, the MCNP input file is read, the geometry position is updated and then transport is performed.

## 6 PROPOSAL

---

As demonstrated by the experiment in chapter ??, the variance reduction parameters generated by the GT-CADIS method are insufficient for optimizing the neutron transport step of SDR analysis in cases that involve the movement of activated components after shutdown. This chapter will first discuss an implementation plan for adding time-integration to R2S and GT-CADIS. This will cover the propagation of error in SDR analysis and discuss some practical considerations for using these methods. Next, a demonstration of these methods will be proposed. Finally, a summary of goals to accomplish will be given.

### 6.1 TR2S

To produce time-integrated SDR maps, the first two steps of the R2S workflow remain unchanged while a photon transport step needs to be performed at each time-step of geometry movement.

1. MC neutron transport simulation on geometry at time step  $t_{\text{mov}} = 0$
2. ALARA activation analysis
3. MC photon transport simulations on geometry at each time step  $t_{\text{mov}} = 1..N$

The MC neutron transport will be performed on the configuration of the geometry during irradiation. A tetrahedral mesh that conforms to the geometry position at  $t_{\text{mov}} = 0$  is used as a tally to score the neutron flux. This mesh is tagged with the geometry transformations that will occur after shutdown. The tetrahedral mesh neutron flux tally along with an irradiation and decay scenario of interest are given as input to the PyNE R2S script to generate ALARA input files. ALARA is run and produces

photon source files for each decay time of interest. These ALARA photon source files are converted to tetrahedral mesh based sources by another PyNE R2S script. All source mesh files generated will reflect the original position of the geometry. Both the source mesh and DAGMC geometry files are transformed to the correct locations for each  $t_{\text{mov}}$  with the DAGMC transform tool.

## 6.2 Implementation: Time-integrated SDR Analysis

This section introduces a plan to generate fully optimized, time-integrated SDR maps. First, a updated R2S workflow that accounts for the movement of activated geometry components after shutdown is discussed. Then, the implementation of the time-integrated solution to the adjoint photon transport derived in chapter ?? is added to the GT-CADIS process of generating the optimal adjoint neutron source.

### 6.2.1 Generation of the TGT-CADIS Variance Reduction Parameters

A CAD model of the geometry in its original position, that during device operation time, is created. This geometry is tagged with transformation numbers corresponding to the stepwise motion vectors that are applied to move the geometry components along the path from their original to final locations. The DAGMC transformation tool discussed in chapter 5 is used to apply the motion vectors and create HDF5 mesh files of the geometry at each time step. The geometry file at each time step along with the adjoint photon source (the flux-to-dose conversion factors) are given as input into a script that generates a Partisn input file. Deterministic

Need to make the distinction between different times. First, there is the decay time,  $t_{\text{dec}}$  which is the amount of time



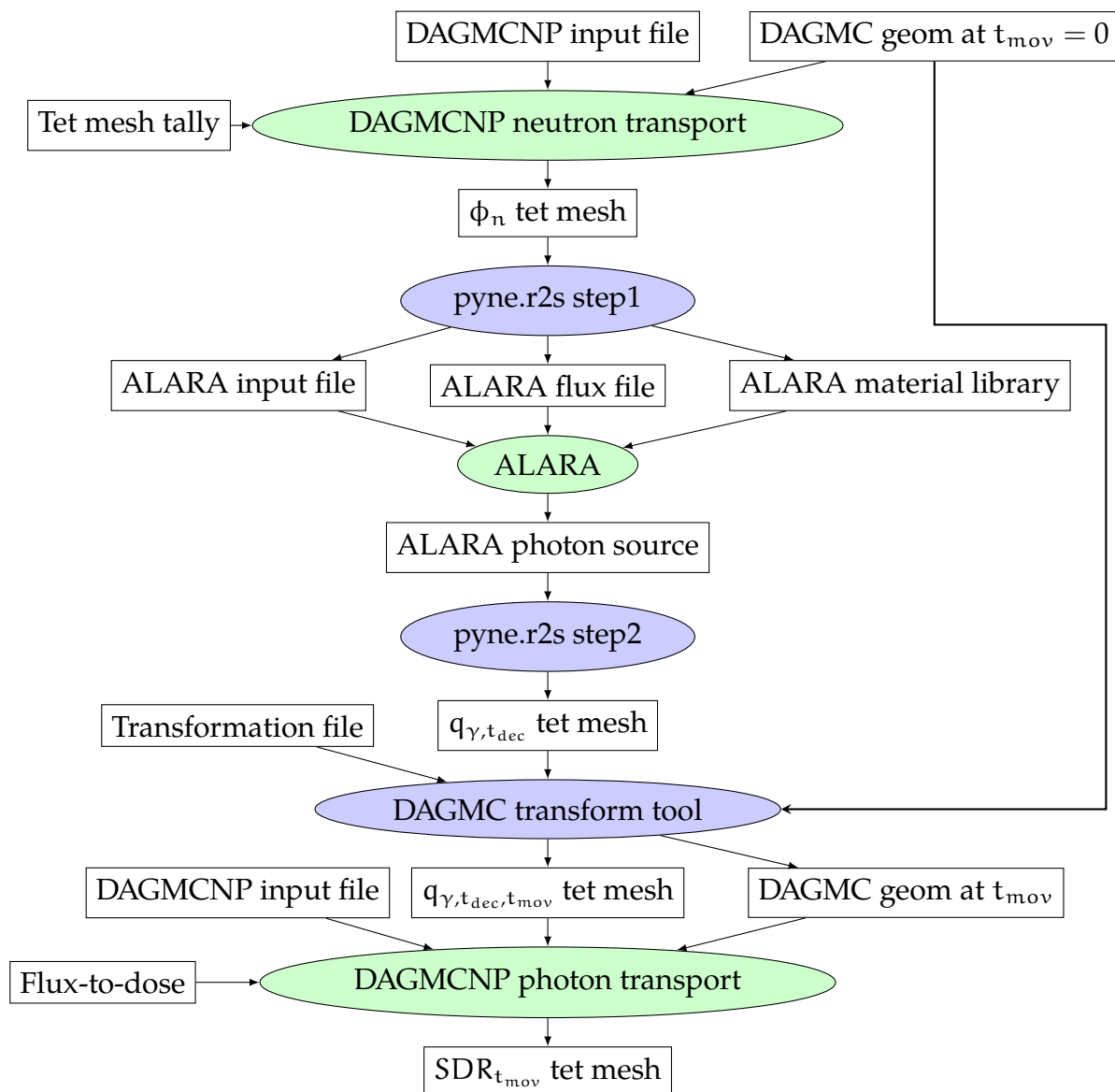


Figure 6.1: Time-integrated R2S (TR2S) workflow for calculating the SDR. Scripts are shown in blue ovals, physics codes in green ovals, and files in white rectangles.

adjoint photon transport is carried out and a Partisn output of the resulting adjoint photon flux is returned. This Partisn output is converted to a an HDF5 structured mesh file through a PyNE conversion method. Because we ultimately need to sum the contribution from each time step in each volume element, the adjoint photon flux voxel mesh is mapped onto the tetrahedral mesh of the geometry at that same time step. Each tet mesh element has an ID associated with it. Those IDs are constant across all geometry files. This allows the contribution of the adjoint flux from each time step to be summed in each tet mesh element.

The time integration is approximated by the following discrete sum over all time steps

$$\phi_{\gamma,v,h}^+ = \sum_{t_{\text{mov}}} \phi_{\gamma,v,h,t_{\text{mov}}} \quad (6.1)$$

The adjoint photon flux tetrahedral mesh is converted back to a voxel mesh to use as input for the PyNE GT-CADIS script. This script ultimately generates a discrete adjoint neutron source for deterministic transport. The coupling term  $T_{g,h}$  is found with Eq. 6.2

$$T_{g,h} = \frac{q_{\gamma,h}(\phi_{n,g})}{\phi_{n,g}} \quad (6.2)$$

To obtain the source of photons in each photon energy group,  $h$ , single pulse irradiations are performed with ALARA. Each material in the problem is irradiated with a single energy group of neutrons,  $g$ , and allowed to decay to the time of interest,  $t_{\text{dec}}$ . The value of  $T_{v,g,h}$  is assigned by finding the material in each voxel,  $v$ . This assumes that  $T$  does not change during the time the geometry is moving,  $t_{\text{mov}}$ .

Combining the calculated  $T$  with the time-integrated adjoint photon

solution, yields the TGT-CADIS adjoint neutron source shown in Eq. 6.3

$$q_{n,v,g}^+ = \sum_{t_{\text{mov}}} \left( \sum_h T_{v,g,h} \phi_{\gamma,v,h,t_{\text{mov}}}^+ \right) \quad (6.3)$$

Once the TGT-CADIS adjoint neutron source has been calculated, deterministic adjoint transport is carried out and an adjoint neutron flux Partisn file is returned. This file is then converted to a voxel mesh. This functions as an importance map for the forward neutron transport. Areas that have a high adjoint neutron flux will have high importance and those with low flux will have low importance. This map will reflect the movement of geometry during the decay period. This adjoint neutron flux mesh is used to generate a biased neutron source and a weight window mesh via the CADIS method.

### 6.2.2 Optimized, Time-integrated R2S Workflow

The source mesh file in its updated position along with the previously generated adjoint photon flux mesh are used to generate a biased photon source and weight window mesh are generated via the CADIS method. At this point, there is a biased photon source mesh, a weight window mesh, and a DAGMC geometry for every time step  $t_{\text{mov}}$ . These are all used along with a DAGMC input file that has a photon flux tally modified by flux-to-dose conversion factors as input for the final DAGMCNP photon transport step. This results in a SDR mesh for each  $t_{\text{mov}}$ .

The TGT-CADIS biased source and weight windows can be used to optimize the neutron transport and the CADIS method can be used to optimize each photon transport step. The fully optimized TR2S implementation is shown in ??.

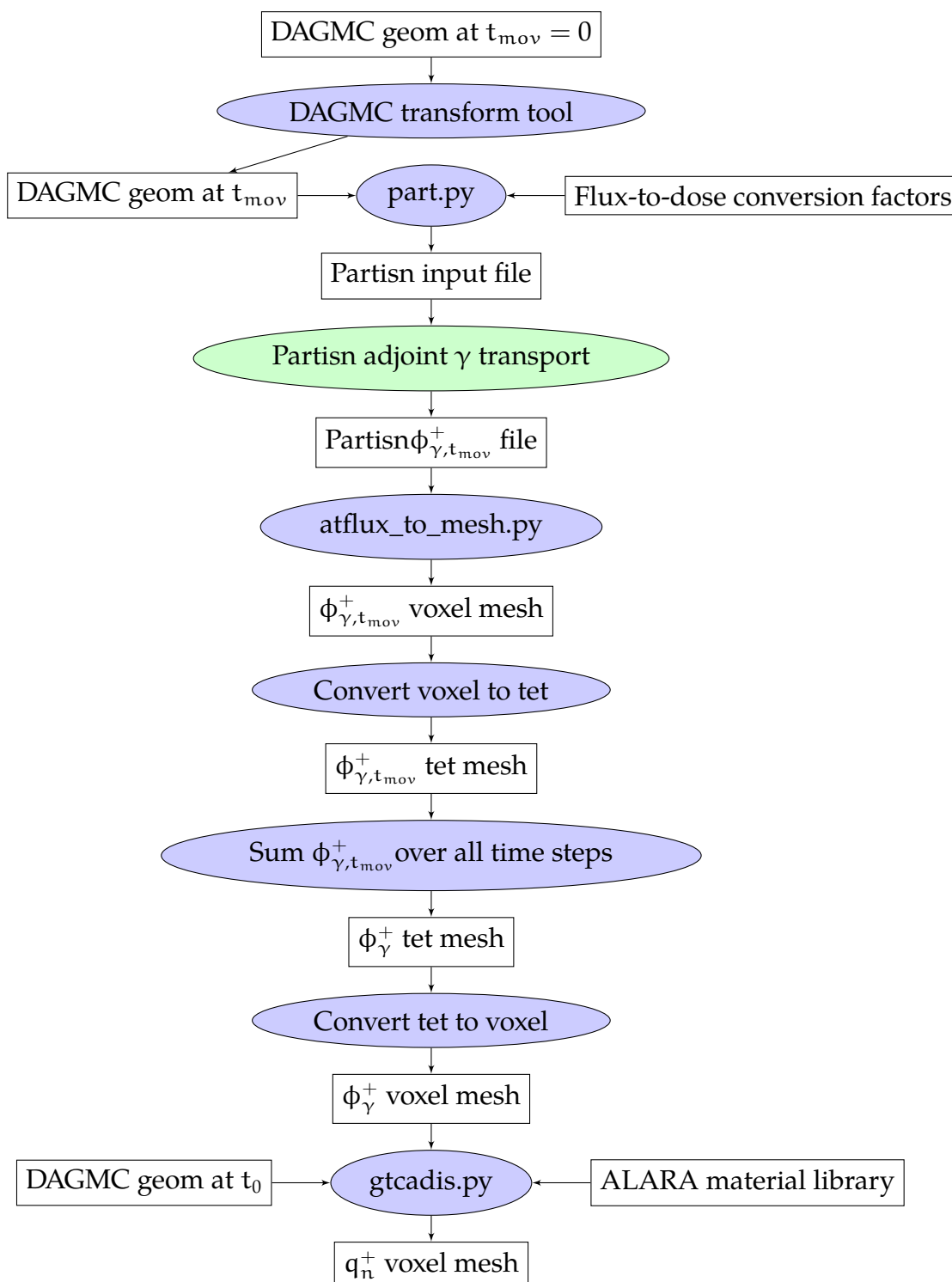


Figure 6.2: Workflow for generating the optimal adjoint neutron source via the time-integrated GT-CADIS method. Scripts are shown in blue ovals, physics codes in green ovals, and files in white rectangles.

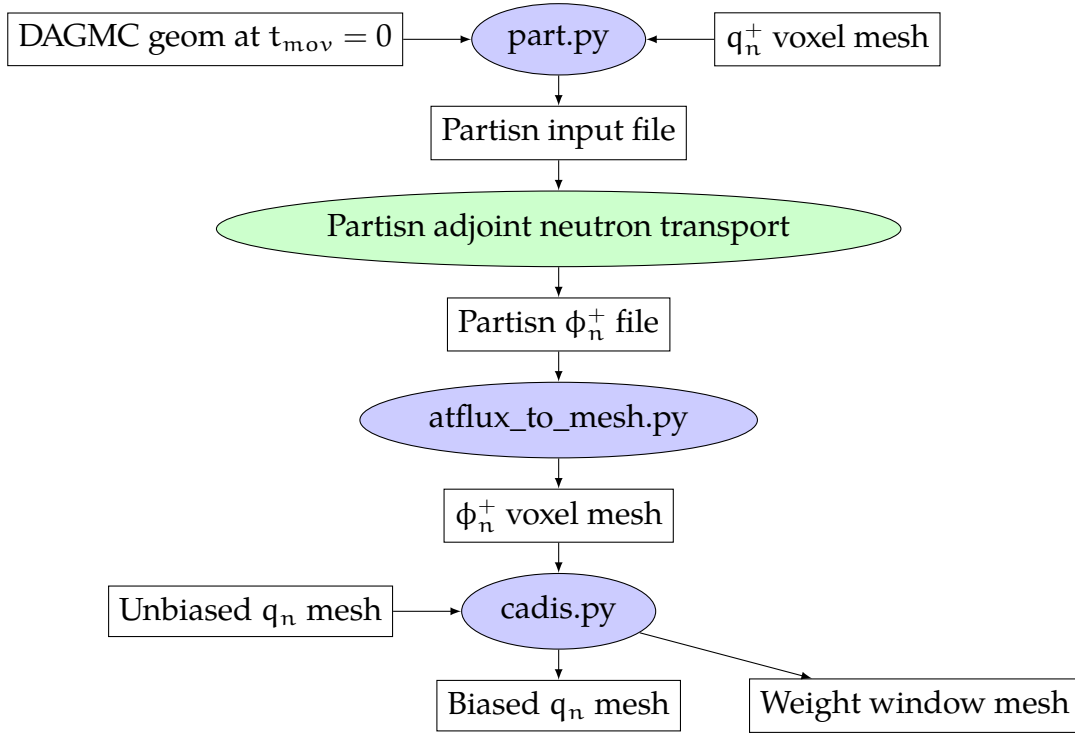


Figure 6.3: Workflow for generating a biased source and weight windows to optimize the neutron transport step. Scripts are shown in blue ovals, physics codes in green ovals, and files in white rectangles.

### 6.2.3 Error Propagation

The total statistical error in the the SDR arises from the MC calculations of the neutron and photon flux.

$$\sigma_{\text{SDR}}^2 = \sigma_n^2 + \sigma_\gamma^2 \quad (6.4)$$

The uncertainty in the SDR due to the uncertainty in the photon transport can be calculated during MC transport. However, the uncertainty in the SDR due to the uncertainty in the neutron MC calculation is more complicated and an area of research currently under investigation by Harb

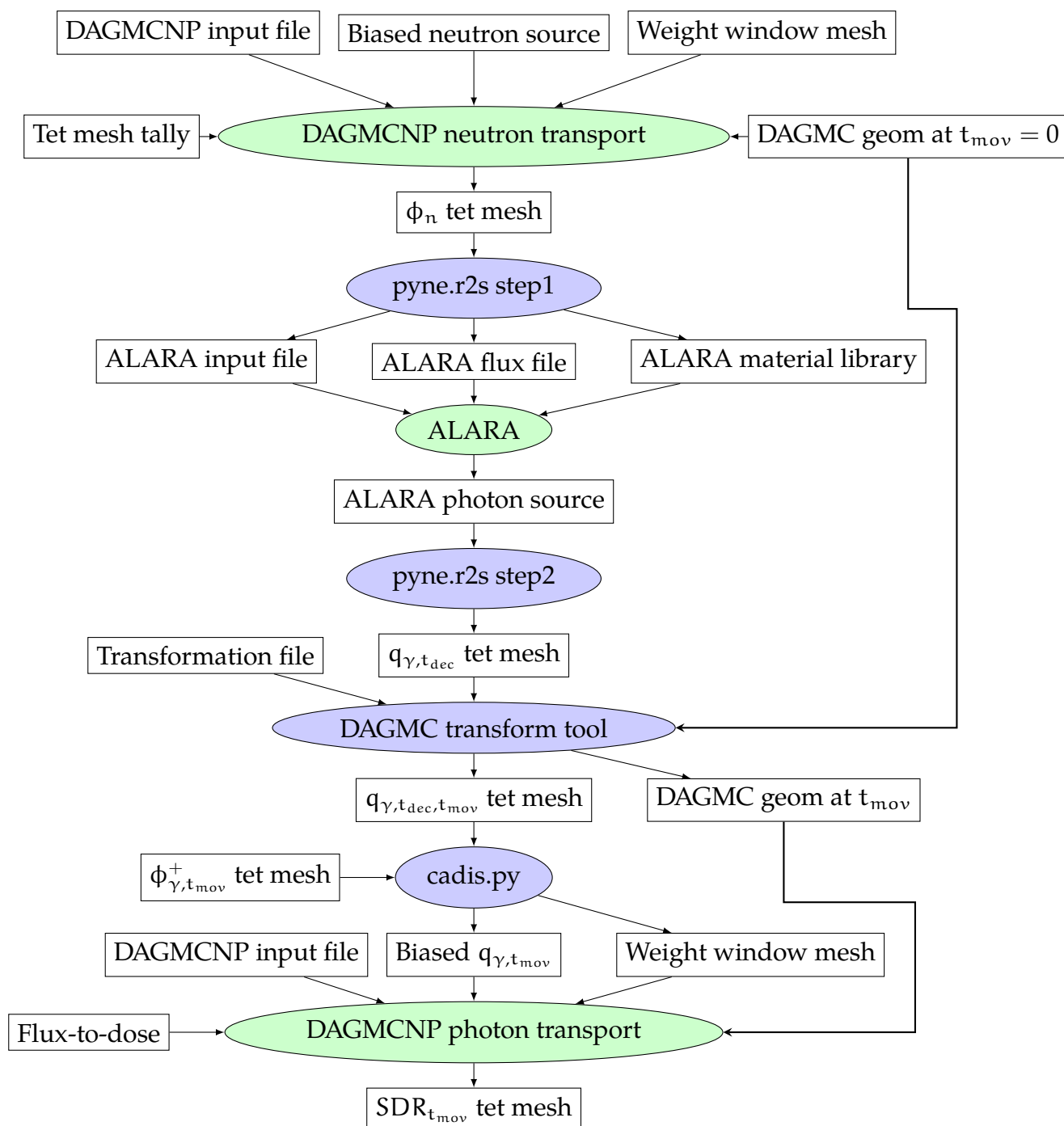


Figure 6.4: Fully-optimized, time-integrated R2S workflow for calculating the SDR. This particular flow chart shows the use of a biased source and weight windows to optimize both neutron and photon transport steps. Scripts are shown in blue ovals, physics codes in green ovals, and files in white rectangles.

et. al. This work aims to produce a methodology for propagating the error from the neutron transport to the photon source and then from the photon source to the SDR.

If a full R2S simulation is carried out, the final SDR has an error associated with the MC neutron photon transport steps. Introducing error from the photon transport step can be avoided by not performing MC photon transport and calculating the SDR using a form of Eq. ??

$$\text{SDR}_v = \phi_{\gamma,v}^+ q_{\gamma,v} \quad (6.5)$$

where  $\text{SDR}_v$  is the response from a discrete volume element,  $v$ . Recall that  $\phi_{\text{gamma},v}$  is the result of the sum of adjoint photon flux over all time steps and required to form the TGT-CADIS adjoint neutron source and  $q_{\gamma,v}$  is the photon source produced by ALARA, so both quantities are already available.

There is some relative error associated with the photon source term that originates from the MC forward neutron calculation. The relative error in the SDR,  $\mathfrak{R}_{\text{SDR}}$  is then expressed as

$$\mathfrak{R}_{\text{SDR}} = \frac{1}{\text{SDR}} \sqrt{\sum_v (\text{SDR}_v \mathfrak{R}_{\text{SDR}_v})^2} \quad (6.6)$$

This error in the SDR can then be used to calculate the neutron transport FOM, shown in Eq. ??, which is important to quantifying the usefulness of TGT-CADIS.

$$\text{FOM} = \frac{\text{SDR}^2}{t_{\text{proc}} \sum_v (\text{SDR}_v \mathfrak{R}_{\text{SDR}_v})^2} \quad (6.7)$$

#### 6.2.4 Assumptions and Practical Considerations

There are three very different time scales: photon transport, geometry movement, and decay. Photon transport happens on a much faster time scale than the geometry movement, therefore it is reasonable to performing

radiation transport on static time-steps of geometry. It is also assumed that the time for the photon emission density to change is much longer than the period of time between the initial and final geometry configurations so the same photon source generated for a particular decay time is used for all photon transport steps  $t_{\text{mov}} = 0..N$ . transport steps during the geometry movement. This also allows the same  $T$  to be used at each time step. Discuss need to explore criteria for situations that this new method will effectively optimize the neutron transport step. It is assumed that the source strength does not change during geometry movement, but a metric will need to be defined to be sure this is true. This depends on the length of time between shutdown and geometry movement. Will need to verify that for a certain window of time, perhaps an eight-hour work shift, the source does not change appreciably. In the case that the source strength is changing appreciably during geometry movement, a series of photon sources that capture these changes over time will need to be used. This will also require the calculation of different  $T$  values for each of these time steps. It is also assumed that the geometry is moving at a constant acceleration and therefore geometry is at each position for an equal amount of time. If this was not true, the sum of adjoint photon fluxes would need to be weighted by time.

#### **6.2.4.1 Data management**

Will be generating a geometry file at each time step, 3-D flux maps for every adjoint photon time step, for the adjoint neutron flux, tet mesh for forward neutron flux, tet mesh of photon source. Need to run adjoint photon transport for many time steps, adjoint neutron, then forward neutron then ALARA.

- efficient obb tree
- htc scripts to run many photon MCNP and compile results



Figure 6.5: Geometry to be used in TGT-CADIS Demonstration.

## 6.3 Demonstration

This section will outline the experiments proposed to demonstrate the utility of TGT-CADIS.

### 6.3.1 Toy Problem

The same geometry used in the GT-CADIS experiment shown in ?? will be used to demonstrate the efficacy of TGT-CADIS. The only difference will be a modular component of the chamber located on the far side of the detector will be moved to a location close to the detector.

First, the TR2S process without any MC VR for the neutron or photon transport steps will be applied to this problem. This will ultimately result in a time-integrated dose map. Next, the photon transport steps will be optimized via the CADIS method. This will require deterministic adjoint photon simulations at each time step to produce VR parameters for the forward MC photon transport runs. Finally, TGT-CADIS will be applied to optimize the neutron transport step. The same adjoint photon flux solutions used in the last step can be used to calculate  $T$  which is then used to calculate the adjoint neutron source for adjoint neutron transport which results in the adjoint neutron flux used to produce the VR parameters.

These incremental additions of optimization will be fundamental in assessing the utility of TGT-CADIS.

### 6.3.2 Full-scale FES Model

As the intended purpose of this work is calculating the SDR during a maintenance or intervention activity in a FES, the final challenge problem

will involve TGT-CADIS optimization of the neutron transport step of TR2S for a full-scale FES.

## **6.4 Summary**

## BIBLIOGRAPHY

---

- [1] A. Haghighat and J. C. Wagner, "Monte carlo variance reduction with deterministic importance functions," *Progress in Nuclear Energy*, vol. 42, no. 1, pp. 25–53, 2003.
- [2] L. Carter and E. Cashwell, *Particle-transport simulation with the Monte Carlo method*. Jan 1975.
- [3] X.-. M. C. Team, *MCNP- A General Monte Carlo N-Particle Transport Code, Version 5*. Apr 2003.
- [4] D. Valenza, H. Iida, R. Plenteda, and R. T. Santoro, "Proposal of shutdown dose estimation method by monte carlo code," *Fusion Engineering and Design*, vol. 55, no. 4, pp. 411 – 418, 2001.
- [5] R. Villari and L. P. Davide Flammini, Fabio Moro, "Development of the advanced d1s for shutdown dose rate calculations in fusion reactors," *Transactions of the American Nuclear Society*, vol. 116, pp. 255–258, 2017.
- [6] Y. Chen and U. Fischer, "Rigorous mcnp based shutdown dose rate calculations: computational scheme, verification calculations and application to iter," *Fusion Engineering and Design*, vol. 63, pp. 107 – 114, 2002.
- [7] J. C. Wagner, D. E. Peplow, and S. W. Mosher, "Fw-cadis method for global and regional variance reduction of monte carlo radiation transport calculations," *Nuclear Science and Engineering*, vol. 176, no. 1, pp. 37–57, 2014.
- [8] A. M. Ibrahim, D. E. Peplow, R. E. Grove, J. L. Peterson, and S. R. Johnson, "The multi-step cadis method for shutdown dose rate cal-

- culations and uncertainty propagation," *Nuclear Technology*, vol. 192, pp. 286 – 298, 2015.
- [9] J. W. Durkee, R. C. Johns, and L. S. Waters, "Mcnp6 moving objects part i: Theory," *Progress in Nuclear Energy*, vol. 87, no. Supplement C, pp. 104 – 121, 2016.
  - [10] J. W. Durkee, R. C. Johns, and L. S. Waters, "Mcnp6 moving objects. part ii: Simulations," *Progress in Nuclear Energy*, vol. 87, no. Supplement C, pp. 122 – 143, 2016.
  - [11] E. D. Biondo and P. P. H. Wilson, "Transmutation approximations for the application of hybrid monte carlo/deterministic neutron transport to shutdown dose rate analysis," *Nuclear Science and Engineering*, vol. 187, no. 1, pp. 27–48, 2017.
  - [12] E. Lewis and W. Miller, *Computational Methods of Neutron Transport*. American Nuclear Society, Inc., 1993.
  - [13] T. Eade, S. Lilley, Z. Ghani, and E. Delmas, "Movement of active components in the shutdown dose rate analysis of the iter neutral beam injectors," *Fusion Engineering and Design*, vol. 98-99, no. Supplement C, pp. 2130 – 2133, 2015. Proceedings of the 28th Symposium On Fusion Technology (SOFT-28).
  - [14] R. ALCOUFFE, R. BAKER, J. DAHL, S. TURNER, and R. WARD, "Partisn: A time-dependent, parallel neutral particle transport code system," may 2005.
  - [15] T. Tautges, P. Wilson, J. Kraftcheck, B. F Smith, and D. Henderson, "Acceleration techniques for direct use of cad-based geometries in monte carlo radiation transport," may 2009.

- [16] ICRP, “Conversion coefficients for use in radiological protection against external radiation,” *ICRP Publication 74. Ann. ICRP*, vol. 26, pp. 3–4.